Liquid–Liquid Two-Phase Mass Transfer in the T-Junction Microchannels

Yuchao Zhao

Dalian Institute of Chemical Physics, Chinese Academy of Sciences, Dalian 116023, China;
and Graduate University, Chinese Academy of Sciences, Beijing 100049, China

Guangwen Chen and Quan Yuan

Dalian Institute of Chemical Physics, Chinese Academy of Sciences, Dalian 116023, China.

In this work, the mass transfer characteristics of immiscible fluids in the two kinds of stainless steel T-junction microchannels, the opposing-flow and the cross-flow T-junction, are investigated experimentally. Water-succinic acid-n-butanol is chosen as a typical example of liquid–liquid two-phase mass transfer process. In our experiments, the mixture velocities of the immiscible liquid–liquid two phases are varied in the range from 0.01 to 2.5 m/s for the 0.4 mm microchannel and from 0.005 to 2.0 m/s for the 0.6 mm microchannel, respectively. The Reynolds numbers of the two-phase mixture vary between 19 and 650. The overall volumetric mass transfer coefficients are determined quantitatively in a single microchannel, and their values are in the ranges of $0.067–17.35\ s^{-1}$, which are two or three orders of magnitude higher than those of conventional liquid–liquid contactors. In addition, the effects of the inlet configurations, the fluids inlet locations, the height and the length of the mixing channel, the volumetric flux ratio have been investigated. Empirical correlations to predict the volumetric mass transfer coefficients based on the experimental data are developed. © 2007 American Institute of Chemical Engineers *AIChE J,* 53: 3042–3053, 2007
Keywords: micromixer, immiscible fluids, microreactor, microfluidic, mass transfer coefficients

Introduction

The importance of microscale devices in chemical engineering has increased significantly within the last decade.[1–4] The extremely large surface-to-volume ratio and the short transport path in microchannels enhance heat and mass transfer dramatically, and hence provide many potential opportunities in chemical process development and intensification. To realize potentials of this new and promising technology, a fundamental understanding of transport processes in micro-channels is necessary. The mass transfer of two immiscible liquids in microscale devices is commonly encountered in chemical and biochemical processes, for instance, in liquid–liquid extraction,[5] nitration,[6] emulsification,[7] etc. Since for the design of microchemical devices, the mass transfer characteristics of the gas–liquid or gas–solid, liquid–liquid systems inside the device have to be known.

The most important work concerning the study of gas–liquid mass transfer in capillaries/microchannels was done by Andersson and coworkers,[8–11] the correlations which they derived to predict the mass transfer coefficients were generally used in monolith reactors system; Berčič and Pintar[12] studied the gas–liquid and liquid–solid mass transfers in capillaries under Taylor flow regime; Qian and Lawal[13]

investigated the slug flow for different geometries and inlet conditions with the numerical simulation in a T-junction microchannel. However, not much was known regarding the simultaneous flow of two immiscible liquids. There was no guarantee that the information available for gas–liquid cases could be extrapolated to liquid–liquid mass transfer, and even little attention had been paid to the immiscible liquid–liquid two-phase mass transfer in microchannels.

In the application areas of mixing and chemical reaction, a number of experimental and numerical studies have been conducted for the T-shaped mixer of larger scales using either liquid or gaseous as working fluids. Tosun[14] studied the micromixing for miscible liquids in T-shaped mixers by using the azo coupling reactions, that the pipe size was roughly equal to 10 mm. Pan and Meng[15] presented an experimental investigation of turbulent flow using PIV and PLIF in a round T-shaped mixer that the diameters of turbulent pipe and round turbulent jet were 76.2 and 12.7 mm, respectively. Zughbi et al.[16] carried out the numerical and experimental investigations of mixing for miscible fluids in pipelines with side and opposing tees by measuring the temperature downstream of a row of heated jets injected into a cold stream. Although many theories, models, and correlations have been developed for miscible fluids mixing and mass transfer in relatively large diameter channels, their applicability to microchannels also needs to be clarified.

Mixing for miscible fluids in the T-shaped microchannels has been studied rather extensively in the recent past and some mixing characteristics of fluids have been explored. Gobby et al.[17] studied the mixing characteristics of two gases in a micro T-mixer by using CFD simulations. Wong et al.[18] fabricated a micro T-shaped mixer in silicon substrate and investigated its feasibility as a rapid mixing microdevice. Woias and coworkers[19,20] carried out numerical and experimental studies on mixing for miscible fluids in micro T-shaped mixer, they highlighted three important flow regimes in the mixing channel, namely, strictly laminar flow, symmetrical vortex flow, and engulfment flow depending on the Re numbers of flow in the mixing channels, it was shown that enhanced mixing performance was achieved with engulfment flow.

A limitation to most of the previous experimental studies of the T-shaped mixer was that they were based on either larger channel size or mixing/mass transfer of two miscible fluids. Although mass transfer in liquid–liquid two-phase flow through microchannel was very important when considering alternatives for process intensification,[21] quantitative investigations were hardly available on the mass transfer characteristics in microchannels for two immiscible fluids. It is not without reason why not much work has been carried out on mass transfer characteristics in micro T-shaped mixers. It had generally been accepted that the hydrodynamics of liquid–liquid two-phase flow in microchannels were not very well understood, especially those involving heterogeneous reactions where mass transfer and chemical reaction compete between themselves in a way. Thorsen et al.[22] demonstrated that microfluidic devices could be used to create controllable droplet emulsions in two immiscible fluids, by injection water into a stream of oil at a T-junction. Guillot and Colin[23] had determined the stability of parallel flows in a microchannel after a T-junction with confocal fluorescence microscopy and identified three typical flow patterns, i.e. droplets formed at the T-

junction, parallel flows, parallel flows which break into droplets inside the channel. Zhao et al.[24] experimentally studied the immiscible liquid–liquid two-phase flow patterns in a T-junction rectangular microchannel by using a CCD camera. They highlighted the flow patterns at the T-junction and in the mixing channel, and the flow patterns map was divided into three zones depending on the superficial Weber numbers of water and kerosene in the mixing channel.

In the present investigation, the main objective is to quantitatively study the mass transfer characteristics of the two immiscible liquid–liquid two phases in well-defined T-junction microchannel systems at different operating conditions. Five-in-series mass transfer zones (namely at the T-junction, in the mixing channel, at the outlet conduit, during the liquid–liquid two-phase droplets falling, during the sampling in the phase separator) are analyzed and investigated, the effects of three latter on the overall mean ka can be minimized or eliminated mathematically by the method of "time extrapolation," so the overall mean ka mainly contains the mass transfer for the T-junction and the mixing channel zones. The mass transfer for various characteristic scales and inlet conditions are also studied. The flow regimes selected for the present investigation are the parallel flow with smooth interface, the parallel flow with wavy interface, the chaotic thin striations flow according to the literature.[24] Deionized water and n-butanol are used as the working fluids, succinic acid as the only diffusing species is transferred from organic to aqueous phase. The overall volumetric mean mass transfer coefficients (ka) of the aqueous phase are obtained.

Theoretical Considerations

The essential features of the T-junction microchannel are shown in Figure 1a. The T-junction microchannel formed by two channel sections joined at a right angle is the simplest microdevice for mixing two fluid streams. Two opposing streams enter coaxially from the two inlet arms and leave through the mixing channel which is perpendicular to the entering direction after colliding at the T-junction. This configuration is called the opposed T-junction micromixer as
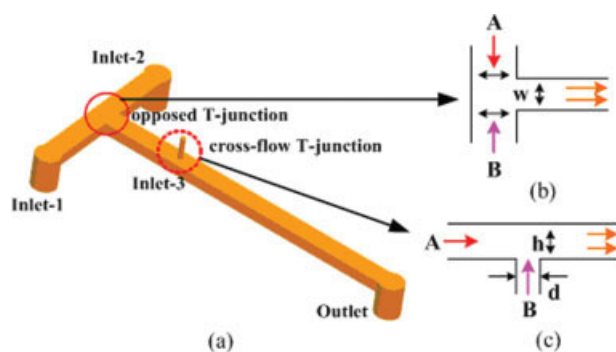
Figure 1. (a) Schematic of the T-junction rectangular microchannel, (b) The opposed T-junction micromixer, inlet-1, and inlet-2 as the inlets, (c) The cross-flow T-junction mixer, inlet-1, and inlet-3 as the inlets.

[Color figure can be viewed in the online issue, which is available at www.interscience.wiley.com.]

Table 1. Dimensions of T-Junction Microchannel Mixers

	Inlet-1 Arm		Inlet-2 Arm		Mixing Channel		Side Channel
	w, μm	h, μm	w, μm	h, μm	w, μm	h, μm	d, μm
Opposed	600	300	600	300	600	300	naught
		600		600		600	
Cross-flow	600	300	naught		600	300	500
		600				600	

shown in Figure 1b. One stream passes straight through the mixing channel and the other enters through the side microchannel and collide the first stream perpendicularly. This configuration is called the cross-flow T-junction micromixer and is shown in Figure 1c. Table 1 shows the actual dimensions of the two kinds of T-junction microchannel mixers.

To accurately determine the overall volumetric mean mass transfer coefficients in the T-junction microchannel system, we must first recognize that there are several fundamentally different mass transfer processes involved. To particularly describe mass transfer processes in the T-junction microchannel system, the entire process is divided into five-in-series mass transfer zones: at the T-junction, in the mixing microchannel, at the outlet conduit, during the liquid–liquid two-phase droplets falling, during the sampling in the phase separator. All these mass transfer zones in the T-junction microchannel system are shown in Figure 2.

From Figure 2, we can see that the entire extraction process of succinic acid encounters five different mass transfer zones in the microchannel system. Each of these mass transfer zones must be separately analyzed relative to the governing relationships within the entire mass transfer process.

T-junction mass transfer zone

In this mass transfer zone, the *n*-butanol and water are all continuous phases during the interphase mass transfer process. The T-shaped junction serves as the contacting unit for liquid–liquid two-phase fluids, the mixing mechanism has an analogy to the confined impinging jets mixing,[25] a high energy dissipation occurs for liquid–liquid two-phase streams because the kinetic energy of each stream is converted into a turbulent-like motion through a collision and redirection of the flow at the T-junction. Engler and coworkers[19,20] numerically studied different laminar flow regimes at the T-junction at different Reynolds numbers, and the laminar flow regimes were divided into three regions,

(a) The stratified flow for low Reynolds number ($Re < 50$), the flow was laminar and the streamlines were straight;

(b) The vortex flow for moderate Reynolds number ($50 < Re < 150$), the symmetrical vortex pair was induced at the T-junction;

(c) The engulfment flow for high Reynolds number ($Re > 150$), the symmetry of the vortex pairs was broken and the streamlines no longer meet in the middle of the channels, but intertwined and reached the opposite side of the wall.

Similarly, three kinds of flow patterns (namely the parallel flow with smooth interface, the parallel flow with wavy interface, the chaotic thin striations flow) were observed at the T-junction of the rectangular microchannel according to

our previous work.[24] Actually, in this work the streamlines no longer meet in the middle of the T-junction zone, but intertwine and reach the opposite side of the microchannel wall. The asymmetrical/chaotic flow which is formed at the T-junction based on geometry and Reynolds number gives an additional interfacial area for liquid–liquid two phases and dramatically enhances the mass transfer process in this zone.

Mixing channel mass transfer zone

The mixing channel is used for further in-line mass transfer enhancement and provides enough residence time needed for chemical reaction or other transformation, as shown in Figure 2. In the mixing channel mass transfer zone, the liquid–liquid two-phase flow regimes intensively depend on the hydrodynamic behavior of two immiscible phases at the T-junction zone. Although three continuous flow patterns could be formed at the T-junction, only two continuous flow patterns remained in the fully developed flow zone (in the mixing channel) because of the viscous friction at the microchannel wall.[24] In our previous work, the symmetrical or asymmetrical vortex and the chaotic thin striations formed at the T-junction zone were transformed to the parallel laminar flow with smooth interface or the annular flow in the mixing channel because the viscous channel wall friction.[24] Because the interfacial area between the two immiscible phases is reduced in this mass transfer zone, the enhancement of the
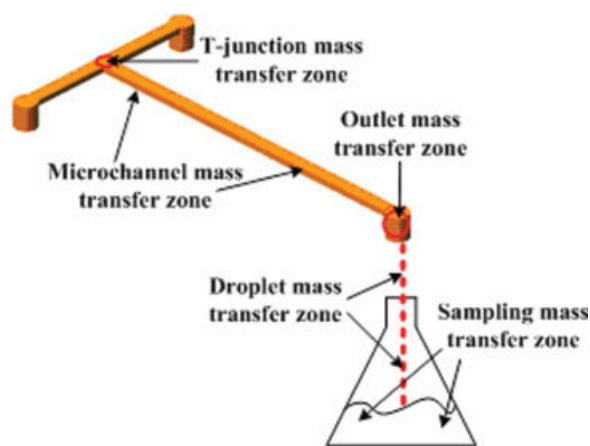
Figure 2. Schematic diagram showing five different mass transfer zones in the T-junction microchannel system with liquid–liquid extraction process.

[Color figure can be viewed in the online issue, which is available at www.interscience.wiley.com.]

mass transfer is weaker than at the T-junction mass transfer zone, however, this weakness is difficult to determine by experiment.

Outlet conduit mass transfer zone

In this mass transfer zone, the outlet conduit formed a 90° angle with the mixing channel having rectangular cross-section, as shown in Figure 2. Analogous to the case of the coiled tubes, the bend can induce secondary circulation that intensifies mass transfer process. As the two immiscible fluids enter the outlet conduit through the bend, the interface between them can stretch, deform, and fold, making the interphase mass transfer more effective. The mass transfer enhancement increases as the Reynolds number increases through the bend of 90° angle. However, viscous effects dominate and the vortices decayed rapidly due to the increasing of the dimensions from the mixing channel to the outlet conduit, the presence of the bend does not contribute significantly to improving mass transfer at very low Reynolds numbers, even the effect of the bend can be neglected compared to the mixing channel mass transfer zone. As we all have known that the shorter the length of outlet conduit, the shorter time for mass transfer process; the larger diameter of the outlet conduit, the higher separation efficiency of two phases achieved or the smaller interfacial area. To minimize the end effects, the specially self-made outlet conduit consisted of the shorter length (20 mm) and larger diameter (5 mm) is employed. Additionally, the interface between the two immiscible fluids decreases dramatically after leaving the microchannel since an order-of-magnitude increase from mixing channel to outlet conduit in the hydraulic diameter. So the additional mass transfer in the outlet conduit zone can be neglected.

Droplets mass transfer zone

In the falling droplets, mass transfer zone, the mass transfer characteristic, and flow patterns of liquid–liquid two phases are difficult to identify. Because the mass transfer in the falling droplets is an unsteady-state process, the flight time of droplets play an important role in the mass transfer in the falling droplets. As the drop height decreases, the flight time of the liquid–liquid two-phase droplets decreases, therefore less succinic acid will be transferred from n-butanol to the aqueous phase. Furthermore, the intensity of disturbance on the surface of the organic phase in the separator can be dampened by the droplets falling from a lower position because less potential energy is converted to kinetic energy that can enhance the mass transfer rate of the surface zone. To minimize the contributions of the falling mass transfer zone, as soon as possible low drop falling height is employed in the experiments.

Sampling mass transfer zone

In the mass transfer zone during sample collection process, the liquid–liquid two-phase droplets from the outlet conduit impinge on the liquid surface of the organic phase in the separator, the phase separation begins to occur and the aqueous phase submerges from the organic phase to the aqueous phase. There is a relatively high velocity and disturbance flow across the entire surface of the organic phase due to the large kinetic energy transformed from the potential energy during droplets falling. The total sampling mass transfer thus includes three processes, namely succinic acid transferred from the surface of the organic phase to the aqueous phase droplets due to the disturbance, the process of submerging from the organic phase to the aqueous phase, and the interface of the two immiscible fluids. Because the time needed for collecting enough sample for analyzing in the separator is usually longer compared to the sum of the residence time at the T-junction, in the mixing channel, in the outlet conduit, and the droplets falling time, thus the mass transfer in the process of sampling must be eliminated.

In all experiments, no difficulties are encountered concerning phase separation. The observation in the separator indicates immediate and complete phase separation during sampling, even for high volumetric flow rate. To eliminate the mass transfer during sampling, the method of "time extrapolation" is employed. At least four different experimental data points are taken in the four different sampling instant intervals. The same experimental data is repeated two times until the standard deviation is in the range of 3.5–5.5%. In all experiments, these experimental data points achieved in all sampling instant intervals are fitted linearly, and the results show that the values of the correlation coefficient R^2 lie in the range between 0.98 and 0.99. Therefore, according to the linear correlation of the extraction efficiency in the sampling mass transfer zone and the sample collection time we can achieve the extrapolated intercept at initial moment, namely, the real extraction efficiency that when the liquid–liquid two-phase droplets arrive at the surface of the organic phase in the separator. So the mass transfer in the sampling mass transfer zone can be eliminated through the method of "time extrapolation."

### Overall volumetric mean mass transfer coefficient

One of our most troublesome points is to respectively determine the individual volumetric mass transfer coefficients by experimenting because the concentrations of solute at the inlet and outlet of the four mass transfer zones are difficult to be known. As mentioned earlier, the mass transfer is described by taking four steps into consideration because the fifth can be eliminated by the method of "time extrapolation." Because the mass transfer processes are in unsteady-state, the individual mean volumetric mass transfer coefficients based on the aqueous volumetric flow rate are normally defined by the following equations.

The T-junction mass transfer zone:

$$k_1 a_1 = \frac{C_{aq,2} - C_{aq,1}}{t_1 \cdot \frac{(C_{aq,1}^* - C_{aq,1}) - (C_{aq,2}^* - C_{aq,2})}{\ln[(C_{aq,1}^* - C_{aq,1})/(C_{aq,2}^* - C_{aq,2})]}} \tag{1}$$

Mixing channel mass transfer zone:

$$k_2 a_2 = \frac{C_{aq,3} - C_{aq,2}}{t_2 \cdot \frac{(C_{aq,2}^* - C_{aq,2}) - (C_{aq,3}^* - C_{aq,3})}{\ln[(C_{aq,2}^* - C_{aq,2})/(C_{aq,3}^* - C_{aq,3})]}} \tag{2}$$
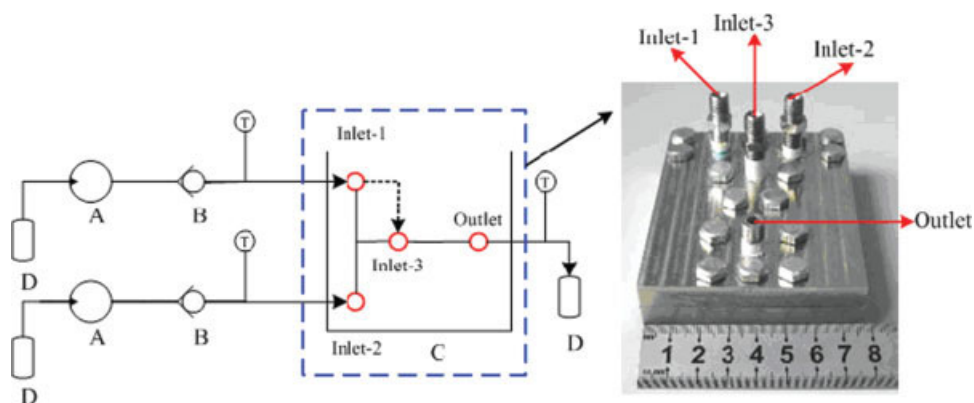
Figure 3. Schematic diagram of experimental setup A: piston pump; B: check valve; C: T-junction microchannel; D: separator.

[Color figure can be viewed in the online issue, which is available at www.interscience.wiley.com.]

Outlet conduit mass transfer zone:

$$k_3 a_3 = \frac{C_{aq,4} - C_{aq,3}}{t_3 \cdot \frac{(C^*_{aq,3} - C_{aq,3}) - (C^*_{aq,4} - C_{aq,4})}{\ln[(C^*_{aq,3} - C_{aq,3})/(C^*_{aq,4} - C_{aq,4})]}} \quad (3)$$

Droplets mass transfer zone:

$$k_4 a_4 = \frac{C_{aq,5} - C_{aq,4}}{t_4 \cdot \frac{(C^*_{aq,4} - C_{aq,4}) - (C^*_{aq,5} - C_{aq,5})}{\ln[(C^*_{aq,4} - C_{aq,4})/(C^*_{aq,5} - C_{aq,5})]}} \quad (4)$$

The concentration profile is discontinuous at the interface of oil and water according to the equilibrium relationship:

$$C_{or,i} = m C^*_{aq,i} \quad (i = 1, 2, 3, 4, 5) \quad (5)$$

The mass balance equation:

$$Q_{or} \cdot C_{or,i} + Q_{aq} \cdot C_{aq,i} = Q_{or} \cdot C_{or,i+1} + Q_{aq} \cdot C_{aq,i+1}$$
$$(i = 1, 2, 3, 4) \quad (6)$$

Therefore, combining Eqs. 1–6, the overall volumetric mean mass transfer coefficient used to describe the mass transfer characteristics of the entire T-junction microchannel system can be rearranged as follows:

$$ka \cdot t = k_1 a_1 \cdot t_1 + k_2 a_2 \cdot t_2 + k_3 a_3 \cdot t_3 + k_4 a_4 \cdot t_4$$
$$= \frac{1}{1 + m^{-1} \cdot \frac{Q_{aq}}{Q_{or}}} \cdot \ln \frac{C^*_{aq,1} - C_{aq,1}}{C^*_{aq,5} - C_{aq,5}} \quad (7)$$

where the superficial residence time of the aqueous phase in the T-junction microchannel system can be calculated by the following equation:

$$t_i = \frac{V_i}{Q_{aq}} \quad (i = 1, 2, 3, 4) \quad (8)$$

$$t = t_1 + t_2 \quad (9)$$

Experimental Section

A schematic diagram of the experimental apparatus is shown in Figure 3. To maintain continuous flow without pul-sation, two piston pumps (Beijing Satellite Manufacturing Factory) and two check valves are used. The aqueous and oil phases are forced to flow through the horizontal rectangular microchannel by these high precision piston pumps, respectively. The mass transfer system is chosen according to the standard test system recommended by the European Federation of Chemical Engineering (EFCE), water-succinic acid-*n*-butanol, as a typical example of liquid–liquid two-phase extraction process.[26] The deionized water is used in all the experiments, which is first boiled in a beaker to remove the dissolved gases and fully degassed. Succinic acid and *n*-butanol are of analytical grade. The organic (*n*-butanol) and aqueous phases (water) are always mutually saturated to prevent multicomponent diffusion in the two phases and hence, succinic acid is the only diffusing species in the mass transfer system. In the present case the concentration of succinic acid in the organic phase is very low (1%), therefore, it is reasonable to assume that the properties of the two immiscible phases are constant in all experimental processes. The present article presents our experimental method and the results from extraction experiments, as well as the mass transfer coefficients calculated using the results.

A calibrated electrical scale with an accuracy of 0.001 g is used to determine the density of saturated aqueous and organic solutions, while temperature is $(22 \pm 1)°C$. The physical properties of water-succinic acid-*n*-butanol system are listed in Table 2.

The T-junction microchannels are fabricated in the stainless steel plate using micromachining technology (FANUC KPC-30a) in our CNC Machining Center. The surface roughness caused by micromachining process, which is in the

Table 2. Physical Properties of Water-Succinic acid-*n*-Butanol System

Mass Transfer System	Density, kg/m³	Viscosity, Pa·s
Saturated deionized water with *n*-butanol	981.69	0.00144
Saturated *n*-butanol with deionized water	837.01	0.00334

At 295 K and atmospheric pressure.

order of several microns, is negligible compared to the characteristic scale for the microchannels in this study.

When the steady state conditions are established, mass transfer runs are made by collecting samples (enough amounts for analyzing) of the outlet streams over measured time intervals. The amount of succinic acid transferred from the organic phase into the aqueous phase is analyzed by titration, using a standard sodium hydroxide solution as the titrant for succinic acid samples. The accuracy of the analytical method is tested by using known samples of aqueous solutions. The maximum error does not exceed ±3%.

Results and Discussion

Definition of parameters

All experiments in the rectangular microchannel are conducted at room temperature and atmospheric pressure. In this article, our main aim is to investigate the overall performance of mass transfer in the T-junction microchannel, therefore, the choice of model for the definition of Reynolds number is determined by the main mass transfer zone. In addition, the flow patterns at the T-junction are different from in the mixing channel. From our previous experimental results about flow patterns[24] and mass transfer performance in Figure 11, we can deduce that the main mass transfer zone is the T-junction zone, so the pseudohomogeneous model fluid model is chosen. The Reynolds numbers of the two immiscible phases can be calculated by the following equations:

$$Re_M = \frac{D_H U_M \rho_M}{\mu_M}, \tag{10}$$

$$D_H = \frac{4A}{2(h+w)}, \tag{11}$$

$$U_M = \frac{Q_{aq} + Q_{or}}{A}, \tag{12}$$

$$\rho_M = \left(\frac{\varphi_{or}}{\rho_{or}} + \frac{1 - \varphi_{or}}{\rho_{aq}}\right)^{-1}, \tag{13}$$

$$\mu_M = \left(\frac{\varphi_{or}}{\mu_{or}} + \frac{1 - \varphi_{or}}{\mu_{aq}}\right)^{-1}, \tag{14}$$

$$\varphi_{or} = \frac{Q_{or}}{Q_{aq} + Q_{or}}, \tag{15}$$

The extraction efficiency is defined as follows[27]:

$$E = \frac{C_{aq,5} - C_{aq,1}}{C^*_{out} - C_{aq,1}} \tag{16}$$

where C^*_{out} is the equilibrium concentration of succinic acid in the outlet aqueous phase. In this work, the mixture velocities of the immiscible liquid–liquid two phases are varied in the range from 0.01 to 2.5 m/s for the microchannel with D_H = 0.4 mm and from 0.005 to 2.0 m/s for the microchannel with D_H = 0.6 mm, respectively.

Flow regimes

The large surface-to-volume ratios of microfluidic devices render surface effects increasingly important, particularly
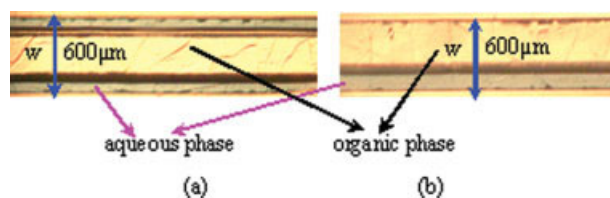
Figure 4. (a) "Sandwich" parallel flow pattern in the cross-flow T-junction (b) "side-by-side" parallel flow pattern in the opposed T-junction.
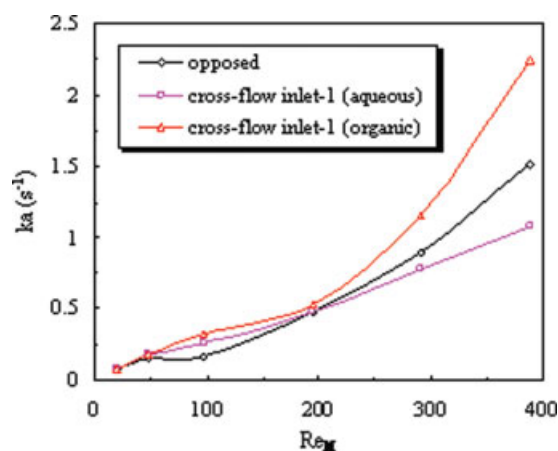
[Color figure can be viewed in the online issue, which is available at www.interscience.wiley.com.]

when free surfaces of two immiscible fluids are present.[28] Surface tensions can exert significant stress that resulting in free surface deformation.[29] Patterned surfaces have been employed in closed microchannels to manipulate multiple immiscible fluids within a single microchannel.[30] It has been confirmed that liquid–liquid two-phase flow structures in microchannel are more seriously affected by the wettability between the channel wall and the fluids. So the flow patterns of liquid–liquid two-phase in steel stainless microchannels can be analogous to PMMA microchannels by controlling surface property. Depending on the T-junction microchannel design, the input oil (n-butanol) volume fraction, mixture Reynolds numbers and the dimensions of microchannel, different liquid–liquid flow regimes are encountered. In our experiments, the organic phase has smaller contact angle than the aqueous phase in the stainless steel microchannel, therefore, the dispersed flow regimes that include slug flow, monodispersed droplets flow, and droplets populations flow are difficult to form. Indeed, we only can observe three flow patterns at the T-junction from our previous work, i.e., the parallel flow with smooth interface, the parallel flow with wavy interface, the chaotic thin striations flow; two flow patterns in the mixing microchannel, i.e., the parallel flow with smooth interface and the annular flow.[24] However, the parallel flow patterns are different for the opposed T-junction microchannel and the cross-flow T-junction microchannel, as shown in Figure 4. The "sandwich" parallel flow pattern and the "side-by-side" parallel flow pattern are formed in the cross-flow T-junction microchannel and in the opposed T-junction microchannel, respectively. As can be seen from Figure 4, the contact area between the immiscible phases in the cross-flow T-junction is larger than that in the opposed T-junction when the flow patterns are parallel flows.

Effect of the different inlet configurations

The effect of the different inlet configurations on the overall volumetric mean mass transfer coefficient (ka) is shown in Figure 5, it appears that the value of ka is found to increase with increasing of Re_M numbers, particularly when Re_M larger than 200. Such a behavior is an increase in the interfacial mass transfer area between the two immiscible phases per unit volume of the microchannel system by the disturbance or chaotic thin striations in the interface of the two phases formed at the T-junction.

From our previous work we know that only three flow patterns can be observed during the similarly investigated range of Reynolds numbers in this work.[24] At low and medium

Figure 5. Effect of the different inlet geometries on the overall volumetric mean mass transfer coefficient $q = Q_{aq}/Q_{or} = 10$, $L = 45$ mm, $w = 600$ μm, $h = 600$ μm, $d = 500$ μm.

[Color figure can be viewed in the online issue, which is available at www.interscience.wiley.com.]

Re_M numbers, the parallel flow with smooth interface and the parallel flow with wavy interface can be observed at the T-junction, both streams flow side by side or sandwich (see Figure 4) through the mixing channel, the disturbance in the interface of the two phases result in a subtle increase in the interfacial mass transfer area between the two immiscible phases per unit volume of the microchannel system in a way. The main mass transfer principle is still diffusion in the interface of the two phases in these flow patterns zone. At higher Re_M numbers, the chaotic thin striations flow pattern which is more efficient for the laminar mixing is induced at the T-junction by the impinging of the two immiscible fluids and centrifugal forces. The interfacial area between two immiscible fluids stretches, deforms, and folds, as well as the surface renewal velocity is enhanced, making the interphase mass transfer more effective, which significantly intensifies mass transfer process and increases the overall volumetric mean mass transfer coefficient. Thus, convection effects and the enlargement of the interfacial area between the two phases play the dominant role on mass transfer in this flow regime.

In addition, as can be seen in Figure 5, at low and medium Re_M numbers, the overall volumetric mean mass transfer coefficient for the opposed T-junction configuration are weak lower than for the cross-flow T-junction configuration. This can be attributed to the larger interfacial mass transfer area for the "sandwich" flow pattern formed at the cross-flow T-junction and in the mixing channel compared to the "side by side" flow pattern formed at the opposed T-junction and in the mixing channel. At higher Re_M numbers, the overall volumetric mean mass transfer coefficient for the opposed T-junction configuration are higher than that for the cross-flow T-junction configuration with the aqueous phase parallel to the mixing channel (the inlet-1 as the inlet for the aqueous phase and the inlet-2 is close, shown in Figure 1), however, lower than that with the aqueous phase perpendicular to the mixing channel (the inlet-3 as the inlet for the aqueous phase). It is thus better to introduce two immiscible fluids head to head or perpendicular to each other with the smaller volumetric flow stream paral-
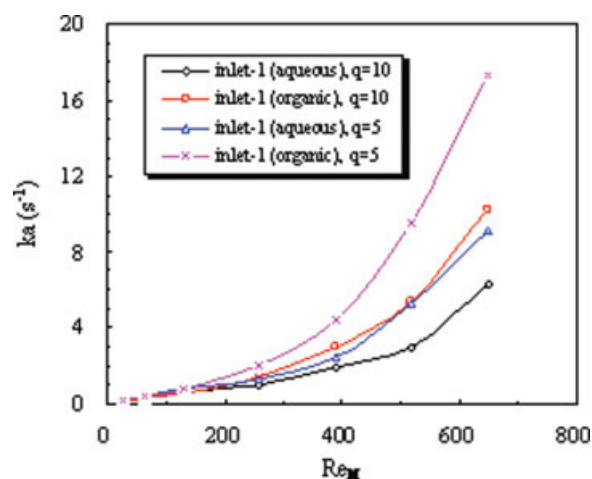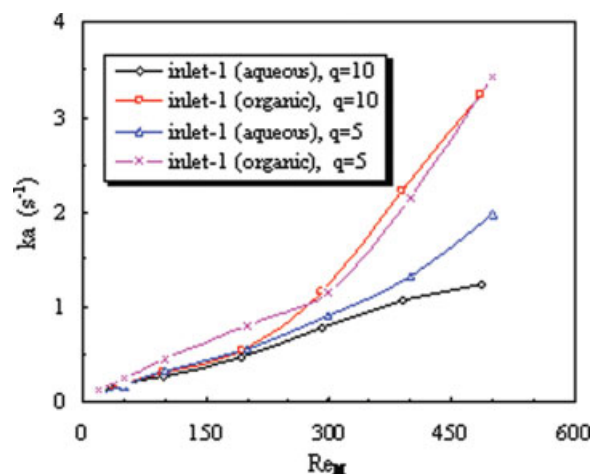

Figure 6. Effect of the fluid inlet locations on the overall volumetric mean mass transfer coefficients in the cross-flow T-junction microchannel, $L = 45$ mm, $w = 600$ μm, $h = 300$ μm, $d = 500$ μm.

[Color figure can be viewed in the online issue, which is available at www.interscience.wiley.com.]

lel to the mixing channel. Perpendicular fluids with the larger volumetric flow rate stream parallel to the mixing channel should be avoided. This behavior may be explained by the difference in the intensity of chaotic thin striations flow due to both the impinging process at the T-junction.

Effect of the fluid inlet locations in the cross-flow microchannel

As stated earlier, the overall volumetric mass transfer coefficients are highly dependent on the fluid inlet configurations. In this section, the mass transfer characteristics in the cross-flow T-junction configuration microchannel will be investigated. Figures 6 and 7 demonstrates the effects of the fluid

Figure 7. Effect of the fluid inlet locations on the overall volumetric mean mass transfer coefficients in the cross-flow T-junction microchannel, $L = 45$ mm, $w = 600$ μm, $h = 600$ μm, $d = 500$ μm.

[Color figure can be viewed in the online issue, which is available at www.interscience.wiley.com.]
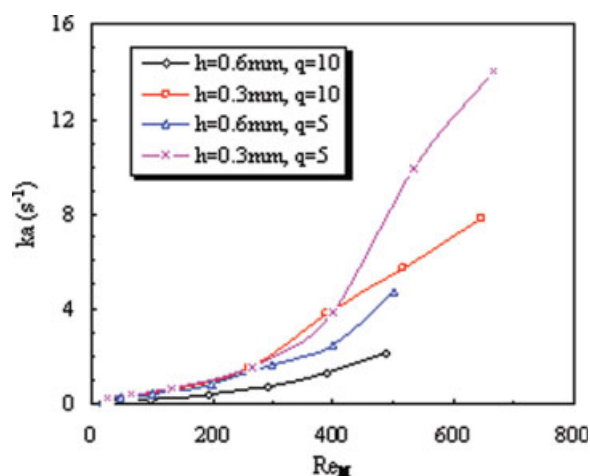
Figure 8. Effect of the depth on the overall volumetric mean mass transfer coefficient in the opposed T-junction microchannel, *L* = 60 mm, *w* = 600 μm.

[Color figure can be viewed in the online issue, which is available at www.interscience.wiley.com.]
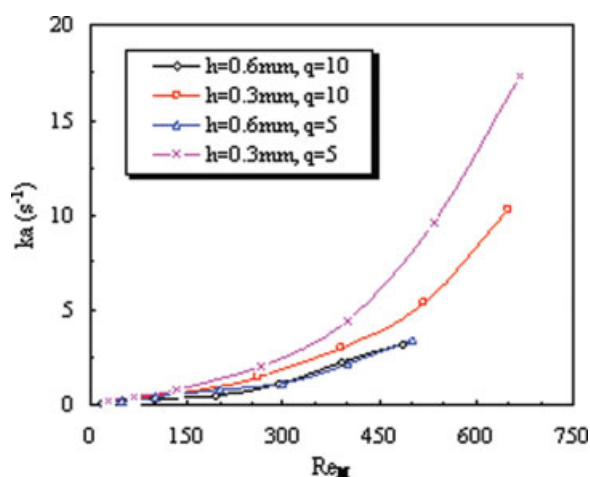
inlet locations on the overall volumetric mass transfer coefficients. Due to its small transverse dimensions (submillimeter), the flow in the mixing channels is typically laminar, and the cross-flow configuration T-junction microchannels provide some different flow characteristics in comparison to the large scale T-mixer.[31] At low Re_M numbers zone ($Re_M < 200$), the stream from the side channel is difficult to penetrate into the mixing channel flow. It attaches to the microchannel wall and flows downstream slowly by the viscous wall friction. The "sandwich" parallel flow with smooth interface is observed at the T-junction, as well as in the mixing channel. The overall volumetric mass transfer coefficients measured are generally small, only a weak increase is observed in this zone (see Figures 6 and 7). Obviously, the flow inlet locations have weak effects on enhancing the mass transfer performance at low Re_M numbers. At medium Re_M numbers zone ($200 < Re_M < 300$), the side flow penetrates into the potential core of the mixing channel flow, turns and aligns with the mixing channel flow. The "sandwich" parallel flows with wavy and smooth interface are observed at the T-junction and in the mixing channel, respectively. At high Re_M numbers zone ($Re_M > 300$), the side flow (aqueous phase) impinges on the opposite wall of the mixing channel and creates a region of backflow or chaotic thin striations, eventually results in larger interfacial mass transfer area and faster surface renewal velocity compared to the organic phase as the side flow. To the same side inlet, it has different volumetric flow-rate when aqueous phase or organic phase is introduced. The aqueous phase has higher kinetic energy according to our operating conditions ($q > 1$). So when it is introduced into the cross-flow inlet, it has more opportunity to impinge on the opposite wall of the mixing channel, and the phenomena of the backflow or chaotic thin striations are prone to occur.

Effect of the height of the microchannel

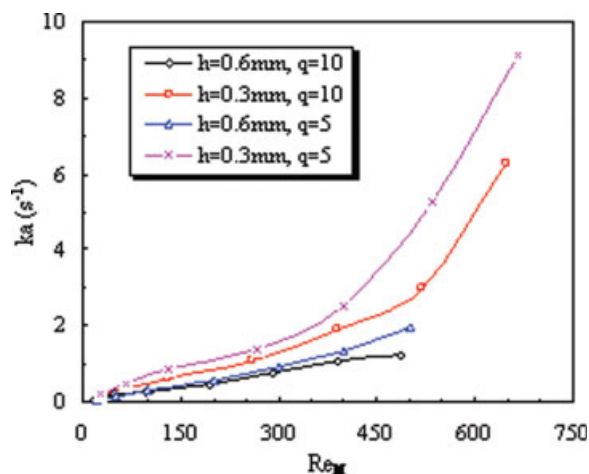The effect of the height on the overall volumetric mean mass transfer coefficients in the opposed T-junction micro-

channel are shown in Figure 8. The mass transfer performance in the microchannel of 300 μm height is significantly improved over the whole Re_M numbers range compared to microchannel of 600 μm height, the effects are more pronounced at higher values of Re_M. This is attributed to an increase in the interfacial mass transfer area and the surface renewal velocity due to the small opposing impinging T-junction space and the increase in the mean flow rate of the two fluids. With a reduction in the height of the microchannel from 600 to 300 μm, the mean flow rates of the two opposing inlets are increased 1.5 times at a constant Re_M number, that is, decreasing the height of the microchannel leads to higher levels of fluid kinetic energy in the opposing impinging T-junction zone. The increase of the mean flow rate in two inlets and the decrease of the opposing impinging T-junction space make the interface of the immiscible fluids disturb or wavy, even chaotic thin striations flow at higher Re_M numbers, which all increase the interfacial mass transfer area and the surface renewal velocity.

Figures 9 and 10 shows the influence of the height on the overall volumetric mass transfer coefficients in the cross-flow T-junction microchannel. The distance from the outlet of the side channel to the opposing wall is reduced two times when the height of the microchannel changes from 600 to 300 μm. This provides an opportunity for the jet from the side channel to significantly penetrate into the potential core of the mixing channel which can result in a weak increase of the interfacial mass transfer area at low Re_M numbers. And the side flow can easily impinge on the opposite wall of the mixing channel and create a region of backflow at high Re_M numbers, thus bigger toroidal vortices can be produced at this small cross-flow zone. This vortex flow is analogous to secondary flow caused in bends by centrifugal forces. As a consequence, the interfacial area of the immiscible fluids and the surface renewal velocity are enlarged, and the mass transfer process is dramatically intensified.

Figure 9. Effect of the depth on the overall volumetric mean mass transfer coefficient in the cross-flow T-junction microchannel, inlet-1(organic), *L* = 45 mm, *w* = 600 μm.

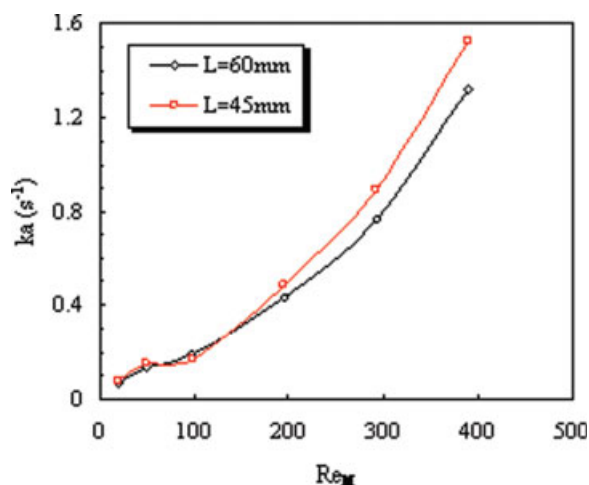[Color figure can be viewed in the online issue, which is available at www.interscience.wiley.com.]

Figure 10. Effect of the depth on the overall volumetric mean mass transfer coefficient in the cross-flow T-junction microchannel, inlet-1(aqueous), $L = 45$ mm, $w = 600$ μm.

[Color figure can be viewed in the online issue, which is available at www.interscience.wiley.com.]

Effect of the length of the microchannel

Figure 11 shows plots of the overall volumetric mass transfer coefficients as a function of the Re_M number under different mixing channel length. It is seen from the plots that the overall volumetric mass transfer coefficients appear to be independent of the length of the mixing channel at lower Re_M numbers, while at higher Re_M numbers the shorter mixing channel demonstrates the higher overall volumetric mass transfer coefficients. This is expected when considering that entrance effects are incorporated into the overall volumetric mass transfer coefficients (Eq. 7). According to the literature,[24] the parallel flow with smooth interface occurs at the

opposed T-junction and in the mixing channel at low Re_M numbers ($Re_M < 200$), thus the interfacial mass transfer area and the surface renewal velocity are almost constant in the microchannel system and the overall volumetric mass transfer coefficients are independent of the length of the mixing channel. While with increasing of the Re_M numbers, the parallel flow with wavy interface and the chaotic thin striations flow are expected to occur at the opposed T-junction, and the two flow patterns are developed into the parallel flow with smooth interface or the annular flow in the mixing channel due to the viscous channel wall friction.[24] And these flow-pattern transitions in the mixing channel can lead to decrease of the interfacial mass transfer area and the surface renewal velocity, namely, the volumetric mass transfer coefficients will be reduced in the fully developed flow in the mixing channel compared to that at the opposed T-junction zone. From the definition of the overall volumetric mass transfer coefficient in Eq. 7, we can see that the mass transfer in the T-junction system is characterized by a mean mass transfer coefficient of all individual mass transfer performance. Thus it is most likely that the entrance effects contribute significantly to this intensification in the mass transfer process. Further work is necessary to study the optimization of the length of the mixing channel and the flow pattern transition mechanism for miniature and process intensification of microchannel systems.

Effect of the volumetric flux ratio

The effects of the volumetric flux ratio ($q = Q_{aq} / Q_{or}$) on the overall volumetric mean mass transfer coefficients are conducted at different Re_M numbers and some of the results are shown in Figures 12 and 13. At low Re_M numbers, the volumetric flux ratio is found to have a weak effect on the overall volumetric mass transfer coefficients. This is mainly due to the low interfacial mass transfer area formed
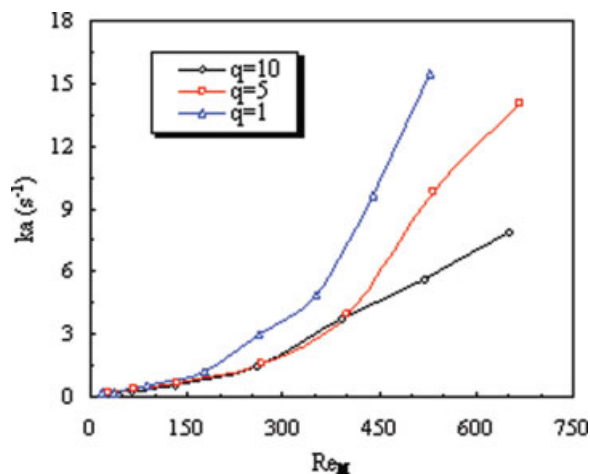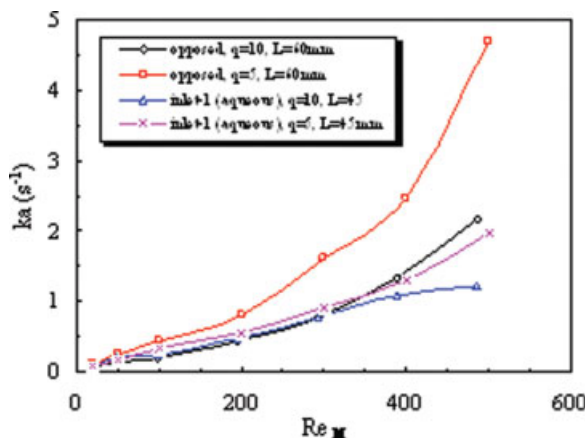

Figure 11. Effect of the length on the overall volumetric mean mass transfer coefficient in the opposed T-junction microchannel, $q = 10$, $w = 600$ μm, $h = 600$ μm.

[Color figure can be viewed in the online issue, which is available at www.interscience.wiley.com.]

Figure 12. Effect of the volumetric flux ratio on the overall volumetric mean mass transfer coefficients in the opposed T-junction microchannel, $w = 600$ μm, $h = 300$ μm, $L = 60$ mm.

[Color figure can be viewed in the online issue, which is available at www.interscience.wiley.com.]

Figure 13. Effect of the volumetric flux ratio on the overall volumetric mean mass transfer coefficients in T-junction microchannel, $w = 600$ μm, $h = 600$ μm.

[Color figure can be viewed in the online issue, which is available at www.interscience.wiley.com.]

at the T-junction and in the mixing channel by the parallel flow with smooth interface. From Figures 12 and 13 we can see that the smaller the volumetric flux ratio, the larger the overall volumetric mass transfer coefficient at medium or higher Re_M numbers, this tendency gradually increases with increasing Re_M number. This can be attributed to the lower kinetic energy ratio of two immiscible fluids at small volumetric flux ratio, because the energy utilization effectiveness in the microchannel system increases with decreasing the volumetric flux ratio. At the same Re_M number, the intensity of disturbance in the interface of two-phase fluids or the chaotic thin striations flow is more dramatically increased for the small volumetric flux ratio compared to the large volumetric flux ratio. As a consequence, the interfacial mass transfer area and the surface renewal velocity are enlarged, which are characteristics for the parallel flow with wavy interface or the chaotic thin striations flow regime and the essential requirements for enhancing mass transfer performance.

Correlation of the Mass Transfer

Liquid–liquid mass transfer process in microchannels is extremely complicated, and no correlation is available to predict the volumetric mass transfer coefficients. Figures 5–13 summarize the effects of the inlet configurations, the fluids inlet locations, the height and the length of the mixing channel, the volumetric flux ratio at different Re numbers on mass transfer. To identify these operating conditions responsible for the overall volumetric mass transfer coefficients in T-junction microchannels, attempts are undertaken to correlate the 92 experimental data points collected during this investigation. The following correlations based on analysis of multiple linear regression are found to predict ka values reasonably well.

For opposed T-junction ($L = 60$ mm):

$$ka = 2.42 \times 10^{-8} \left(1 + \frac{1}{q}\right)^{0.27} Re_M^{0.87} D_H^{-1.65} \quad Re_M < 200 \tag{17}$$

$$ka = 1.92 \times 10^{-12} \left(1 + \frac{1}{q}\right)^{1.22} Re_M^{2.16} D_H^{-1.94} \quad Re_M > 200 \tag{18}$$

For cross-flow T-junction ($L = 45$ mm) and inlet-1 (aqueous):

$$ka = 2.61 \times 10^{-8} \left(1 + \frac{1}{q}\right)^{1.31} Re_M^{0.83} D_H^{-1.65} \quad Re_M < 200 \tag{19}$$

$$ka = 1.47 \times 10^{-11} \left(1 + \frac{1}{q}\right)^{2.61} Re_M^{1.85} D_H^{-1.85} \quad Re_M > 200 \tag{20}$$

For cross-flow T-junction ($L = 45$ mm) and inlet-1 (organic):

$$ka = 3.28 \times 10^{-6} \left(1 + \frac{1}{q}\right)^{4.05} Re_M^{0.84} D_H^{-0.97} \quad Re_M < 200 \tag{21}$$

$$ka = 3.21 \times 10^{-11} \left(1 + \frac{1}{q}\right)^{2.31} Re_M^{2.17} D_H^{-1.56} \quad Re_M > 200 \tag{22}$$

Figure 14 demonstrates the experimental values of ka vs. the predicted values by Eqs. 17–22. The correlations predict the data, with a deviation of 20%. The details of regression parameters based on analysis of multiple linear regression are shown in Table 3. From these correlations we can observe the relative importance of the parameters on the mass transfer process in different channel configurations and operating conditions. This agrees well with earlier discussion that the mass transfer process can be intensified by the larger Reynolds number ($Re_M > 200$), the inlet configurations and the smaller channel scale.

Comparison with Other Kinds of Contactors

To assess the potential of the T-junction microchannel contactor, the volumetric mass transfer coefficients are compared with other large scaled liquid–liquid contactors in Figure 15, where the volumetric mass transfer coefficient values are taken from pictures or tables presented in literatures[32–34] and from Figures 5–13 in this article, respectively. The overall volumetric mass transfer coefficient is the most important param-
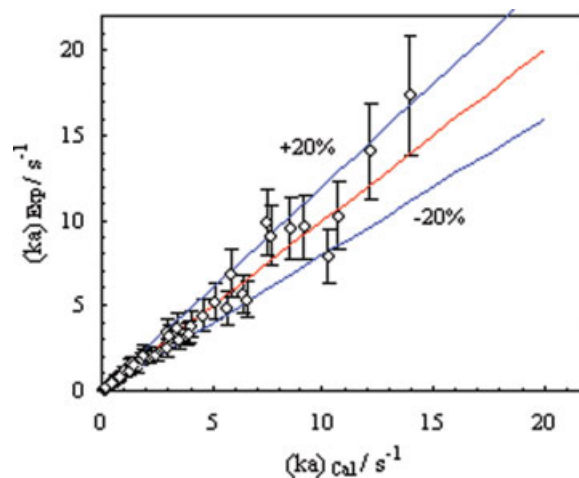
Figure 14. Comparison between experimental and predicted ka values.

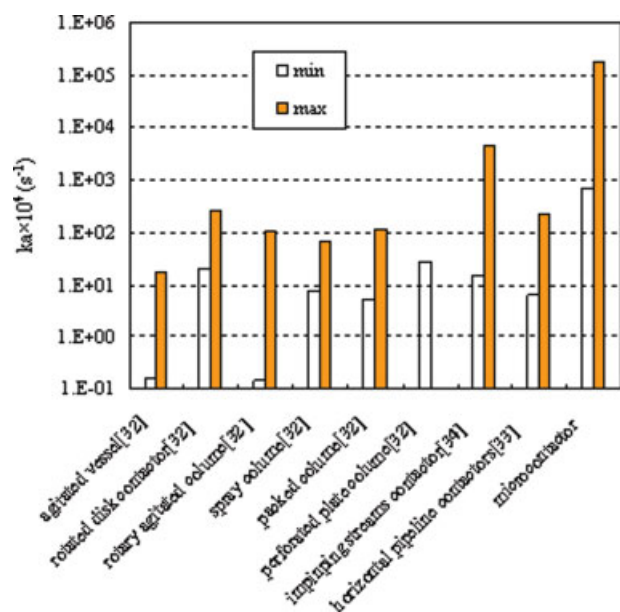[Color figure can be viewed in the online issue, which is available at www.interscience.wiley.com.]

Table 3. Regression Parameters Based on Analysis of Multiple Linear Regression

$\tilde{q}$	$\tilde{s}$	$\tilde{r}$	$\tilde{v}_i$			$\tilde{u}$	Eqs.
			$1+1/q$	Re_M	D_H		
0.49	0.15	0.98	0.51	0.999	0.999	15.2	(17)
0.35	0.15	0.983	0.938	0.999	0.999	9.73	(18)
0.064	0.063	0.997	0.95	0.999	0.999	11.3	(19)
0.21	0.13	0.985	0.944	0.999	0.999	6.95	(20)
0.026	0.043	0.998	0.997	0.999	0.999	6.78	(21)
0.24	0.13	0.986	0.93	0.999	0.999	8.65	(22)

$\tilde{q}$, $\tilde{s}$, $\tilde{r}$, $\tilde{v}_i$, and $\tilde{u}$ represent sum of square of deviations, average standard deviation, multiple correlation coefficient, partial correlation coefficient, and regression sum of square, respectively.

eter in liquid–liquid/gas–liquid contactors. To examine the practical use of the T-junction microchannel contactor, eight kinds of large scaled liquid–liquid contactors are chosen to compare the performance with the T-junction microchannel contactor based on the values of the overall volumetric mean mass transfer coefficient. Actually, it is difficult to accurately compare the performance of this T-junction microchannel contactor with the corresponding literature data for other contactors since it is essential that the experiments be conducted using systems with identical interfacial characteristics, under the same operating conditions, and the results interpreted using consistent parameters, thus the effects of these different conditions on the overall volumetric mean mass transfer coefficient should be taken into account accurately.

From Figure 15 we can see that the overall volumetric mass transfer coefficients obtained in the present investigation are more than two or three orders of magnitude higher than those liquid–liquid large scaled contactors,[32–34] so the volume of microchannel contactor reduction similar magnitude or more can be achieved. Although columns and other

Figure 15. Comparison of the liquid–liquid contactors.

[Color figure can be viewed in the online issue, which is available at www.interscience.wiley.com.]

traditional liquid–liquid contactors have been workhorses of the chemical industry for decades, an important disadvantage is the interdependence of the two fluid phases to be contacted, which sometimes leads to difficulties such as emulsions, foaming, unloading and flooding. Advantages microchannel contactors offer over other mass transfer equipment include the following:

(a) the combined effect of the above mentioned factors resulting in significant reduction in the microsystem's volume which results in major reduction of the capital cost requirements (equipment, foundations);

(b) large interfacial mass transfer area for microchannel contactors can be achieved;

(c) the maintenance and operation is relatively simple;

(d) the cocurrent mode of operation can avoid the flooding;

(e) the emulsion phenomenon almost not occurs and the separation efficiency is higher;

(f) short and narrow time residence distribution;

(g) suitability for limited spaces and easiness of incorporation in existing processes;

(h) unlike the conventional contactors, no density difference is required between fluids;

(i) scale-up is more straightforward with microchannel contactors;

(j) high throughput and high space-time yield.

However, the microchannel contactors has a vital disadvantage, namely, the microchannels are subject to fouling. These relatively few disadvantages are often outweighed by the numerous advantages cited above. For this reason, microchannel contactors have attracted the attention of many interested parties from both academia and industry for a diverse range of applications.

Conclusions

The mass transfer characteristics of the T-junction microchannel contactors are investigated by measuring the overall volumetric mean mass transfer coefficient. Some important results obtained are as follows:

(1) The entire mass transfer process is divided into five-in-series mass transfer zones: mass transfer at the T-junction, in the mixing microchannel, in the outlet conduit, during the liquid–liquid two-phase droplets falling, the sampling intervals in the phase separator. And the mass transfer in the sampling intervals can be eliminated by the method of "time extrapolation."

(2) The different inlet configurations, the fluids inlet locations and Reynolds numbers play an important role in the mass transfer process.

(3) A decrease in the height or the length of the mixing channel at constant Re_M number results in an increase in the overall volumetric mean mass transfer coefficients.

(4) The overall volumetric mean mass transfer coefficients increase by decreasing the volumetric flux ratio.

(5) Empirical correlations are developed based on the obtained data representing Reynolds numbers and inlet configurations. These correlations can predict the volumetric mass transfer coefficients with deviation of $\pm 20\%$.

(6) Compared with the other liquid–liquid contactors reported on the overall volumetric mass transfer coefficients, the T-junction microchannel contactor can significantly enhance the mass transfer process.

Acknowledgments

Notation

a = interfacial area, m^2/m^3

A = cross-sectional area of microchannel, m^2

$C_{aq,i}$ = concentration of the solute of the inlet aqueous phase at i (i = 1,2,3,4,5) mass transfer zone, kg/m^3

$C^*_{aq,i}$ = equilibrium concentration of the solute of the inlet aqueous phase in i (i = 1,2,3,4,5) mass transfer zone corresponding to the actual inlet concentration of the solute in the organic phase, kg/m^3

$C_{or,i}$ = concentration of the solute of the inlet organic phase in i (i = 1,2,3,4,5) mass transfer zones, kg/m^3

d = diameter of the side microchannel, m

D_H = hydraulic diameter of microchannel, m

E = extraction efficiency

h = microchannel height, m

k = overall mean mass transfer coefficient, m/s

ka = overall volumetric mean mass transfer coefficient, 1/s

L = channel length, m

m = partition coefficient of solute between aqueous and organic phases

$q = Q_{aq} / Q_{or}$ = volumetric flux ratio

Q = volumetric flow rate, m^3/s

t_i = superficial residence time of the aqueous phase in i (i = 1,2,3,4) mass transfer zone, s

U_M = mixture velocities of the immiscible liquid–liquid two phases, m/s

V_i = volume of i (i = 1,2,3,4) mass transfer zone, m^3

w = microchannel width, m

Re_M = mixture Reynolds number of the immiscible liquid–liquid two phases

Greek letters

μ = viscosity, Pa s

ρ = mass density, kg/m^3

φ = hold-up fraction

Subscripts

aq = aqueous phase

i = location of the microchannel system

M = mixture of the immiscible liquid–liquid two phases

or = organic phase

1 = the T-junction

2 = the mixing channel

3 = the outlet conduit

4 = the falling droplets

5 = the sampling

Literature Cited

1. Ehrfeld W, Hessel V, Löwe H. *Microreactor*. New York: Wiley/VCH, Weinheim, 2000.

2. Jensen KF. Microreaction engineering—is small better? *Chem Eng Sci*. 2001;56:293–303.

3. Jähnisch K, Hessel V, Löwe H, Baerns M. Chemistry in microstructured reactors. *Angew Chem Int Ed*. 2004;43:406–446.

4. Chen GW, Yuan Q, Li HQ, Li SL. CO selective oxidation in a microchannel reactor for PEM fuel cell. *Chem Eng J*. 2004;101:101–106.

5. Tokeshi M, Minagawa T, Uchiyama K, Hibara A, Sato K, Hisamoto H, Kitamori T. Continuous-flow chemical processing on a microchip by combining microunit operations and a multiphase flow network. *Anal Chem*. 2002;74:1565–1571.

6. Burns JR, Ramshaw C. A microreactor for the nitration of Benzene and Toluene. *Chem Eng Commun*. 2002;189:1611–1628.

7. Willaime H, Barbier V, Kloul L, Maine S, Tabeling P. Arnold tongues in a microfluidic drop emitter. *Phys Rev Lett*. 2006;96:054501.

8. Hatzlantoniou V, Andersson B. Solid-liquid mass transfer in segmented gas-liquid flow through a capillary. *Ind Eng Chem Fundam*. 1982;21:451–456.

9. Irandoust S, Andersson B. Mass transfer and liquid-phase reactions in a segmented two phase flow monolith catalytic reactor. *Chem Eng Sci*. 1988;43:1983–1988.

10. Irandoust S, Andersson B, Bengtsson E, Siverström M. Scaling up of a monolithic catalyst reactor with two-phase flow. *Ind Eng Chem Res*. 1989;28:1489–1495.

11. Irandoust S, Ertle S, Andersson B. Gas-liquid mass transfer in Taylor flow through a capillary. *Can J Chem Eng*. 1992;70:115–119.

12. Berčič G, Pintar A. The role of gas bubbles and liquid slug lengths on mass transport in the Taylor flow through capillaries. *Chem Eng Sci*. 1997;52:3709–3719.

13. Qian DY, Lawal A. Numerical study on gas and liquid slugs for Taylor flow in a T-junction microchannel. *Chem Eng Sci*. 2006;61:7609–7625.

14. Tosun G. A Study of micromixing in Tee mixers. *Ind Eng Chem Res*. 1987;26:1184–1193.

15. Pan G, Meng H. Experimental study of turbulent mixing in a Tee mixer using PIV and PLIF. *AIChE J*. 2001;47:2653–2665.

16. Zughbi HD, Khokhar ZH, Sharma RN. Mixing in pipelines with side and opposed Tees. *Ind Eng Chem Res*. 2003;42:5333–5344.

17. Gobby D, Angeli P, Gavriilidis A. Mixing characteristics of T-type microfluidic mixers. *J Micromech Microeng*. 2001;11:126–132.

18. Wong SH, Ward MCL, Wharton CW. Micro T-mixer as a rapid mixing micro-mixer. *Sens Actuators B*. 2004;100:359–379.

19. Engler M, Kockmann N, Kiefer T, Woias P. Numerical and experimental investigations on liquid mixing in static micromixers. *Chem Eng J*. 2004;101:315–322.

20. Kockmann N, Kiefer T, Engler M, Woias P. Convective mixing and chemical reactions in microchannels with high flow rates. *Sens Actuators B*. 2006;117:495–508.

21. TeGrotenhuis WE, Cameron RJ, Butcher MG, Martin PM, Wegeng RS. Microchannel devices for efficient contacting of liquids in solvent extraction. *Sep Sci Technol*. 1999;34:951–974.

22. Thorsen T, Roberts RW, Arnold FH, Quake SR. Dynamic pattern formation in a vesicle-generating microfluidic device. *Phys Rev Lett*. 2001;86:4163–4166.

23. Guillot P, Colin A. Stability of parallel flows in a microchannel after a T junction. *Phys Rev E*. 2005;72:066301.

24. Zhao YC, Chen GW, Yuan Q. Liquid-liquid two-phase flow patterns in a rectangular microchannel. *AIChE J*. 2006;52:4052–4060.

25. Johnson BK, Prud'homme RK. Chemical processing and micromixing in confined impinging jets. *AIChE J*. 2003;49:2264–2282.

26. Misek T, Berger R, Schröter J (ed). *Standard Test Systems for Liquid Extraction*, 2nd edition. EFCE Publications Series No. 46. Warwickshire: The Institution of Chemical Engineers, 1985.

27. Saien J, Zonouziana SAE, Dehkordi AM. Investigation of a two impinging-jets contacting device for liquid-liquid extraction processes. *Chem Eng Sci*. 2006;61:3942–3950.

28. Squires TM, Quake SR. Microfluidic: fluid physics at the nanoliter scale. *Rev Mod Phys*. 2005;77:977–1026.

29. Eggers J. Nonlinear dynamics and breakup of free-surface flows. *Rev Mod Phys*. 1997;69:865–929.

30. Zhao B, Moore JS, Beebe DJ. Surface-directed liquid flow inside microchannels. *Science*. 2001;291:1023–1026.

31. Sroka LM, Forney LJ. Fluid mixing with a pipeline Tee: theory and experiment. *AIChE J*. 1989;35:406–414.

32. Laddha GS, Degaleesan TE. *Transport Phenomena in Liquid Extraction*. Tata McGraw-Hill: New Delhi, 1976.

33. Shah AK, Sharma MM. Mass transfer in liquid-liquid (horizontal) pipeline contactors. *Can J Chem Eng*. 1971;49:596–604.

34. Dehkordi AM. Novel type of impinging streams contactor for liquid-liquid extraction. *Ind Eng Chem Res*. 2001;40:681–688.